JOURNAL OF MATERIALS SCIENCE 32 (1997) 6001–6008

Room temperature synthesis of crystalline metal oxides

M. GOPAL*,§, W. J. MOBERLY CHAN§ and L. C. De JONGHE*,§
*Department of Materials Science and Mineral Engineering, University of California, Berkeley CA 94720, USA
§Center for Advanced Materials, Lawrence Berkeley National Laboratory, Berkeley CA 94720, USA

Crystalline titanium dioxide powders have been synthesized as either rutile or anatase from aqueous solutions at low temperatures ($T \leqslant 100\,^{\circ}C$) and atmospheric pressure. First, a sol is prepared by the hydrolysis of a titanium alkoxide in an acidic solution. The sol is subsequently heated at different rates to produce the different crystalline phases of titanium dioxide. Powder characterization was carried out using X-ray diffraction, scanning electron microscopy and high resolution transmission electron microscopy. In general, the precipitate size was observed to be between 50 and 100 nm. Possible mechanisms involved in determining the crystal variants are discussed.

1. Introduction

Titanium dioxide is utilized as a pigment, an enamel, a synthetic gem, an ingredient in welding rod coatings and as a catalyst. In the electronics industry, the rutile form of titania is used for its high dielectric constant and high electrical resistance. It has, therefore, found application in capacitors, filter and power circuits and temperature compensating condensers. Titania is also an important starting component in the preparation of mixed oxides (such as barium and strontium titanates), which in turn exhibit ferroelectric behaviour [1]. Porous titania coatings and membranes are also desirable for artificial photosynthesis [2], as separators [3] and as catalysts [4].

Several methods have been developed to synthesize TiO_2. These include decomposition of $TiOSO_4$ [5], calcination of titanyl hydroxide [6], oxidation of titanium trichloride ($TiCl_3$) [7] and titanium tetrachloride ($TiCl_4$) [8], hydrolysis of $TiCl_4$ [9, 10], titanium alkoxide [11] and titanium hydroxide [12]. The disadvantages of most processing methods are the use of corrosive chemicals and/or high temperatures to obtain the desired crystalline oxide.

Room temperature (or near room temperature $T \leqslant 100\,^{\circ}C$) synthesis of crystalline oxide particles eliminates the need for high temperature operations. The benefits of room temperature processing are enhanced when the chemicals are sufficiently benign to facilitate the processing in air. One class of starting compounds that provide the possibility of obtaining crystalline oxide at room temperature are metal alkoxides. These compounds have the generic formula $M(OR)_z$, where R is an alkyl group and z is the valency of the metal, M. The OR groups are electronegative and therefore make the metal highly prone to nucleophilic attack. The metal alkoxides react with water, leading to the formation of amorphous hydroxides and hydrous oxides, which in turn can be converted to crystalline oxide by heating. This sol–gel processing route has been widely exploited to make ceramic parts [13].

The reaction between alkoxide and water has been extensively studied and generally can be considered as a two step process – a hydrolysis reaction and a consideration (or polymerization) reaction [14]. Hydrolysis occurs upon the addition of water and results in the formation of an M–OH bond. The subsequent condensation reaction can occur once the OH groups are created. Depending on the experimental conditions, either alcohol or water is the by-product. The structure and morphology of the resulting oxide network depends on both internal parameters (nature of the alkyl group, structure of the molecular precursor, etc.) and the external parameters (water/alkoxide ratio, temperature, catalyst, solvent, concentration, etc.) [15].

The rationale behind the approach to synthesize crystalline phases directly from alkoxides, is based on the assumption that complete hydrolysis needs to occur before the condensation reaction begins. If condensation starts before completion of hydrolysis, alkyl groups are incorporated into the structure [16] and sterically hinder the formation of ordered structures. It is further presumed that condensation should proceed slowly for the molecules to crystallize into an equilibrium structure. A faster reaction rate will result in either amorphous or metastable structures. Complete hydrolysis followed by slow condensation can be effected by processing at a low pH. Acidic solutions enhance the rate of hydrolysis [14], because the OR groups attached to the metal are protonated by

H_3O^+, making their charge more positive. Since the metal ions are positively charged, they repel the OR group and attach to OH groups, thus promoting hydrolysis. (A small number of OR groups may remain in the structure, in equilibrium with the ROH in the solution; this has been observed at neutral pH [17]). Not only does acid promote hydrolysis, it also causes a marked decrease in the rate of condensation [14]. This is because the protonated species repel each other, thereby decreasing their interaction.

Acid-catalysed reactions have been widely studied [18, 19] and have been employed to make coatings [20] and monoliths [21]. As with most sol–gel processes, the precipitate must be heated to about 1000 °C to form a crystalline product. We report a process by which two of the crystalline phases of TiO_2 can be synthesized directly in an aqueous solution near room temperature.

2. Experimental procedure

TiO_2 was synthesized in a mixture of distilled water, nitric acid and 2-propanol (Baker Chemical Co., Phillipsburg, NJ), and titanium isopropoxide (Aldrich, Milwaukee, WI). The chemicals were used as received from the manufacturer without further purification with concentrations as listed in Table I. The water to alkoxide ratio was very large (1000:1) compared to the 1:1 ratios typical in sol–gel synthesis.

Water and nitric acid were first mixed at room temperature, and then 2-propanol was slowly added. After the solution was thoroughly mixed, titanium isopropoxide was gradually added with a pipette. Gelatinous white precipitates were instantly formed. The mixture was ultrasonically agitated, and after about 5 min became clear and transparent indicating the formation of a sol. This sol was heated to give titanium dioxide precipitates. The following heating schedules were adopted; (a) constant temperature; heating from 23 to 35 °C at about 0.5 °C min^{-1}, and holding at 35 °C. Cloudiness, indicating precipitation, appeared after 7.5 h. (b) Slow heating (0.5 °C min^{-1}). Cloudiness appeared at 62 °C after 75 min. (c) Intermediate heating (2 °C min^{-1}). Cloudiness appeared at 79 °C after 29 min. (d) Fast heating (5 °C min^{-1}). Cloudiness appeared at 90 °C after 16 min.

Phases were identified by both X-ray and electron diffraction. For the X-ray diffraction studies, the precipitates were allowed to settle for 24 h. Then, the majority of the liquid was removed with a pipette, and the powder was dried under an infra-red heat lamp (maximum temperature ~90 °C). The dried precipitate was ground with a mortar and pestle to a fine powder for the analysis in the X-ray diffractometer (Siemens, Kristalloflex Diffraktometer).

The morphology of the precipitates was studied by scanning electron microscopy (SEM). The precipitates were separated from the solution by centrifuging and washed several times with methanol to remove residual alkoxides. A drop of the suspension was placed on the SEM specimen holder, dried, rinsed with methanol to remove any contamination, and observed in the SEM (ICI-DS 130C).

TABLE I Concentration of chemicals used in the synthesis

Chemical	Concentration of stock	Quantity added (ml)	Moles
Water	Distilled	72	5
Nitric acid	5 moles per litre	10	0.05
Titanium isopropoxide	Pure	1.5	0.005
Isopropyl alcohol	Pure	5	0.065

For transmission electron microscopy (TEM; Topcon-002B), the precipitates were collected on holey carbon grids (Ted Pella Inc) suspended vertically in the stirred solution processed at 40 °C. Three time intervals for acquiring specimens were chosen: from 2 to 2.5, 5 to 5.5, and 7 to 7.5 h. After removal, the grids were washed in distilled water and isopropyl alcohol and dried for 30 min under a heat lamp.

3. Results and discussion

3.1 Crystal structure

The X-ray diffraction patterns in Fig. 1 illustrate the effect of the heating rate on the phase formation. The maximum temperature reached for any of the processing conditions was less than 100 °C. When the solution was held at a constant 35 °C or under slow heating (samples A and B), rutile was formed. For intermediate rates of heating (sample C), both rutile and anatase was formed. When the heating rate was fast (sample D), primarily anatase was formed. The results of these experiments are summarized in the approximate

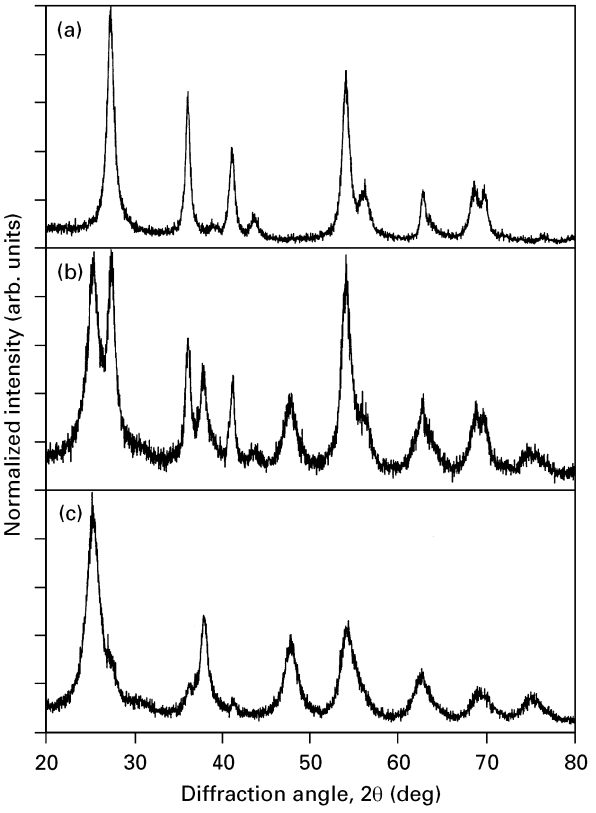

Figure 1 Effect of heating rate on the phase formed. (a) Samples A and B (slow heating rate) are rutile, (b) sample C (intermediate heating rate) is a mixture of anatase and rutile and (c) sample D (fast heating rate) is anatase.

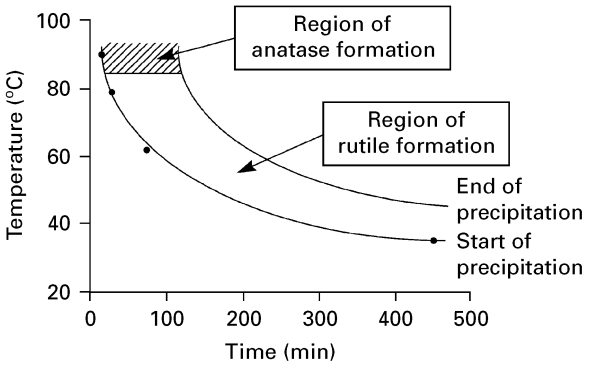

Figure 2 An approximate time–temperature–transformation diagram for the formation of crystalline titanium dioxide. The lower line indicates the start of the precipitation process as determined visually, the black circles corresponding to experimentally determined points. The higher line represents the end of the precipitation process.

time–temperature–transformation diagram shown in Fig. 2.

3.1.1 Precipitation mechanism

Titania can naturally occur in three mineral forms: anatase, rutile, and brookite [8]. Anatase and rutile both have tetragonal structures, whereas brookite is orthorhombic. The experimental Ti–O phase diagram indicates that anatase is more stable than rutile at room temperature and atmospheric pressure [22]. However, thermodynamic data show that anatase is metastable with respect to rutile under all conditions of temperature and pressure [23]. All three crystal structures consist of (TiO_6^{2-}) octahedra, which share edges and corners in different manners, but such that the overall stoichiometry is TiO_2. The structures of rutile and anatase are presented in Fig. 3 (a and b) [24]. In rutile, two opposite edges of each octahedra are shared forming a linear chain along the (0 0 1) direction. Chains are then linked to each other by sharing corner oxygen atoms. Anatase has no corner sharing, but has four edges shared per octahedron. The anatase structure can be viewed as zigzag chains of octahedra, linked to each other through shared edges. Although anatase has more edge sharing, the interstitial spaces between octahedra are larger, thereby making it less dense than rutile (density of rutile is 4.26 and of anatase is 3.84 $g\,cm^{-3}$ [25]). The structure of brookite is more complex [26] and is not discussed here, as it was not part of our synthesis programme.

While the final crystal structures have 6-fold Ti-co-ordination, the titanium has 4-fold co-ordination in the initial alkoxide precursor [$Ti(OR)_4$]. However, when the alkoxide reacts with water, the metal ion increases its co-ordination by using its vacant d-orbitals to accept oxygen lone pairs from nucleophilic ligands (such as OH groups) by co-ordination expansion [14]. Consequently, titanium ions in solution exist as 6-fold co-ordinated structures. The composition of this solution structure $Ti(O)_a(OH)_b(OH_2)_{6-a-b}$ where a and b depend on the processing conditions. Since the reaction is performed in an

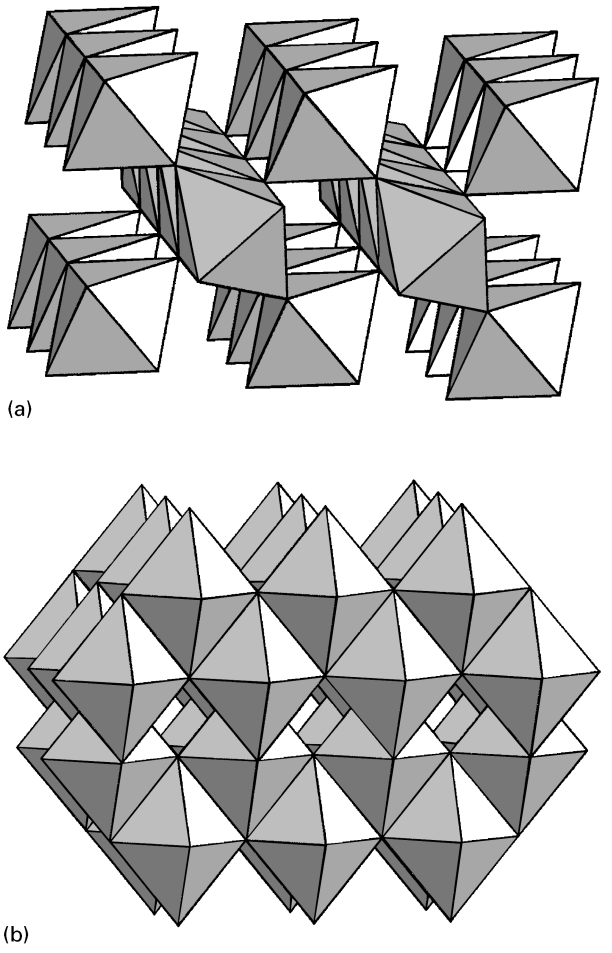

Figure 3 Arrangement of octahedra in (a) rutile and (b) anatase.

acidic medium, only $-OH_2$ and –OH groups will be present, thus the composition reduces to $[Ti(OH)_x(OH_2)_{6-x}]^{(4-x)+}$ [27]. These six-fold structural units undergo condensation and become the octahedra that are incorporated into the final precipitate structure.

The octahedra agglomerate through corner and edge sharing during the condensation reactions. Face sharing does not occur in the titania system because of strong repulsion between the $+4$ charged metal ions. In a neutral solution, the aggregation is rapid and the precipitate appears amorphous by X-ray diffraction. However, work of others using small angle X-ray diffraction indicates that the precipitates have "short-range order" similar to that in anatase [28] or brookite [29]. The existence of this short range order is further substantiated by the observation that amorphous gels produced from alkoxides first convert to anatase instead of forming the more stable rutile structure [30].

In the present study, the hydrolysis and condensation reactions occur at a low pH. The alkoxide, upon contacting water, forms a white precipitate. The acid causes proton absorption on the surface of these precipitates making them positively charged. The point-of-zero-charge (PZC) of this compound is at pH = 6.8, hence a lower pH value promotes the charging process [3]. The resulting electrostatic repulsion causes larger particles to break down into smaller particles until an

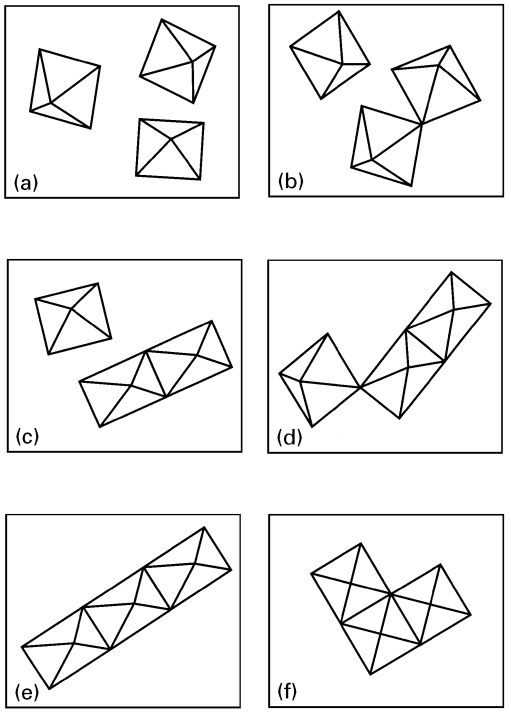

Figure 4 Proposed mechanism for the formation of rutile and anatase. (a) Isolated octahedra in solution; (b) two octahedra join at a vertex; (c) octahedra join along an edge. Cation–cation repulsion causes distortion; (d) third octahedron joins the cluster at a corner; (e) linear array-fundamental structural unit of rutile and (f) right angle array-fundamental structural unit of anatase. The rutile phase is thermodynamically more stable as the octahedra are in a linear array minimizing the electrostatic repulsive energy. The anatase phase is however statistically favoured as there are more edges the third octahedron can bond to and form a right-angled array.

equilibrium size is reached. At this stage, the particles are sufficiently small such that little light scattering occurs, and the suspension becomes an optically transparent sol. The size of the particles in this sol has been estimated to range from 8 [31] to 100 nm [28].

Since the initial reaction product of alkoxide and water is an amorphous aggregate, it is expected that the titania sol particles are also amorphous. When this amorphous sol is heated (or even aged at room temperature), crystalline precipitates are obtained. A plausible mechanism for crystallization can be inferred from the work of Kumar *et al.* [4]. When these workers process the amorphous titania sol by heating, they obtain anatase. However, when they heat the sol in the presence of SnO_2 nuclei, rutile is formed. They attribute this to the nucleation and growth of rutile on SnO_2 as the lattice mismatch between the two structures is small. These results suggest that the crystallization actually occurs by single octahedra of titania dissolving from the sol, and reprecipitating. In the present study, alkoxides have been employed to synthesize rutile without a seed crystal.

The dependence of the phase formed on the reaction rate can be considered using simple reaction-rate concepts in which rutile, anatase, and possibly random structures nucleate in competition. In a simple nucleation model, the higher thermodynamic stability for rutile will lead to a lower activation energy. Qualitatively, one should expect that the respective nucleation activation energies, Q, would order as $Q_{\text{rutile}} < Q_{\text{anatase}} < Q_{\text{amorphous}}$. This sequence will correspond to a preferred formation of rutile at lower temperatures, with an increasing tendency to form anatase at increased processing temperatures, as was observed here.

A mechanism by which this may occur is proposed schematically and sequentially in Fig. 4 (a–f). Two octahedra that are free in solution (Fig. 4a), undergo a condensation reaction and initially join at a corner (Fig. 4b). Upon further condensation, the two will become joined along an edge (Fig. 4c). When this happens, the cation–cation repulsion causes the centres of the two octahedra to move apart, and the shared edge becomes shorter [32]. The placement of the third octahedron determines whether a rutile or an anatase nucleus is formed. The third octahedron initially joins the two-octahedron cluster at a corner (Fig. 4d). Then two options exist: to bond such that the three octahedra are in a line (basic structural unit of rutile – Fig. 4e), or to bond such that a right-angle is formed (basic structural unit of anatase – Fig. 4f). The linear configuration (rutile) is thermodynamically favourable because it allows the largest cation–cation distances. However, the configurations that are possible with three joined octahedra statistically favour anatase. Hence, faster reaction rate favours anatase formation.

An additional consideration is that restructuring of the forming nucleus may also be involved. Transformation of the tri-octahedral nucleus to a rutile configuration would involve a diffusional rearrangement after initial clustering. Such a process is in many aspects similar to diffusion-limited particle cluster aggregation such as discussed by Meakin [33], where denser structures result upon more extensive diffusion. In order of decreasing density one has rutile–anatase–random. Increased precipitation rates, e.g., as a result of increased supersaturation, can then be expected to lead to a similar sequence of phase formation, favouring rutile formation at the slowest precipitation rates.

3.2 Morphology of precipitates

The initial stage of particle formation, which controls the crystal structure, results in the formation of primary crystallites. These primary crystallites subsequently coalesce and form precipitates. The resulting morphologies and methods by which the precipitates are formed are discussed below.

SEM imaging of rutile precipitates (after 12 h of reaction) depicts needle-shaped features which are $\sim$70 nm in length. The needles in turn have agglomerated to form spheroids, which are upwards of 200 nm (Fig. 5a). On the other hand, the synthesized anatase precipitates (Fig. 5b) exhibit much smaller sizes, nominally less than 50 nm in size. Although the anatase precipitates also agglomerate, the resulting larger structures are irregular. The observation that anatase grains are smaller than rutile is also reflected in the broad anatase peaks observed in the X-ray diffraction data (Fig. 1).

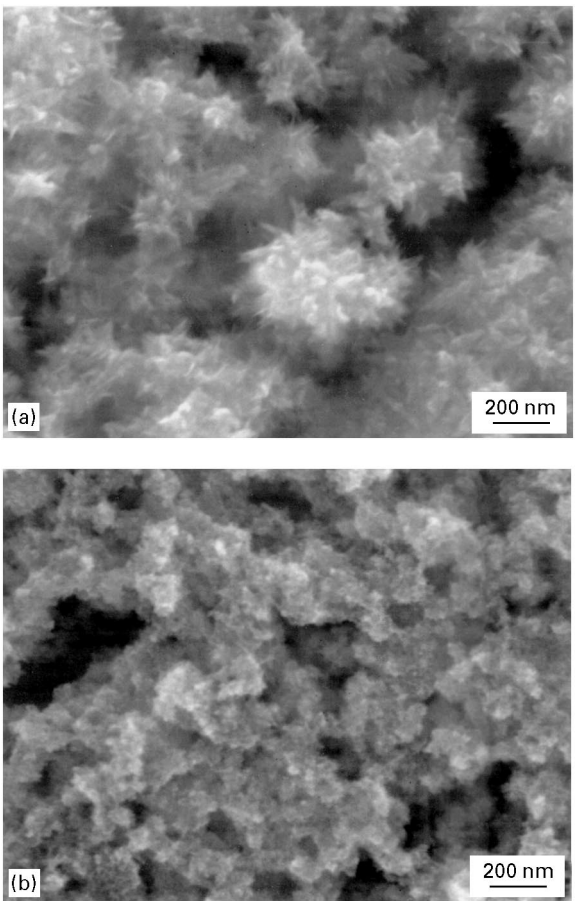

Figure 5 Scanning electron micrographs of (a) rutile and (b) anatase. The image of rutile shows spheroidal aggregates of needle shaped precipitates. The image of anatase precipitates shows finer precipitates that have aggregated into larger irregular structures.

Fig. 6 (a and c) shows TEM images of the precipitates as they develop during processing. Fig. 6b, which is an electron diffraction ring pattern, determines that the precipitates are rutile. The sharpness of the (0 0 2) ring corresponds to the needles being elongated in the [0 0 2] direction; while the higher-than-theoretical intensity of the (0 0 2) ring corresponds to the propensity for the needles to lie on the holey-carbon TEM substrate. Fig. 6 (a and c) are dark-field images from the specimens prepared in the time intervals of 2 to 2.5 h and 7 to 7.5 h respectively. These images show the needles increase in size as the reaction proceeds. Table II lists the sizes of the particles measured from dark field TEM images. The dark-field images show that individual needles are comprised of smaller particulates, ~ 3 nm in size. It is important to note that in each needle, all the particulates diffract together or they all do not, indicating a common crystallographic orientation. Fig. 6d is a bright-field image corresponding to Fig. 6c. The high resolution lattice image (Fig. 6e) exhibits (1 1 0) rutile fringes extending the length of the precipitate. The discontinuities in the cross fringes are due to the needle-shaped precipitates being comprised of an aggregation of small (< 3 nm) crystallites.

The needle-like precipitates are formed by the aggregation of the primary crystallites which, as indicated by the dark field TEM images (Fig. 6 (a and c)), are about 3 nm in size. The aggregation occurs along specific crystallographic directions, resulting in precipitates with long-range order. Since the observed precipitates are made up of smaller crystallites, they can be termed "colloidal crystals" [34]. Such an ordering mechanism was first proposed in the gelation of clays [35] and has been extended to explain the formation and growth of V_2O_5 [36, 37] and ZrO_2 [38]. Some factors that have been proposed to explain ordered aggregation are non-uniform surface charge distribution and anisotropy of the hydration layer [39]. These forces could cause the aggregation to proceed such that the overall energy is minimized. Aggregation therefore occurs preferentially along the *c*-axis as it is the direction of high surface energy for the rutile structure [26]. However, the aggregation process never allows perfect low energy (1 1 0) facets to develop. Thus the needles do not develop long parallel sides as occur in the slow natural mineral formation of rutile. Instead, the needles develop a compromised oblong shape.

As the number density of needle-like precipitates in the solution increases at a later stage of the process, the needles agglomerate into spheroids, as imaged by SEM (Fig. 5a) and TEM (Fig. 7a). Although the SEM image suggests spheroids are dense dendritic particles, TEM determines they are polycrystalline and not dense. The spotted ring pattern in the selected area diffraction pattern from one cluster, Fig. 7b, determines that the cluster contains a random collection of needles. High resolution TEM lattice imaging, Fig. 7c, of the boxed area in Fig. 7a determines that each individual needle has a single crystalline orientation, but again is comprised of numerous smaller crystallites. The 0.148 nm spacing of the (0 0 2) rutile planes are not readily resolved because of distortions associated with the aggregation of crystallites.

The aggregation processes which lead to the formation of needles and spheroids of rutile are functions of both the ageing time and the density of the particles. Both aggregation processes are promoted by longer time and higher particle densities (which occurs with longer time). These crystallites are produced rapidly and therefore do not have sufficient time to form large ordered crystals.

3.3. Role of other processing parameters

Two additional processing parameters that could influence the synthesis of oxides are the alcohol concentration and the type of acid. In this study, the

TABLE II Particle size (in nm) as a function of processing time period as measured from dark field TEM images

	Largest		Average	
	Length	Width	Length	Width
2–2.5 h	30	6	10	3
5–5.5 h	50	11	20	5
7–7.5 h	71	16	40	7

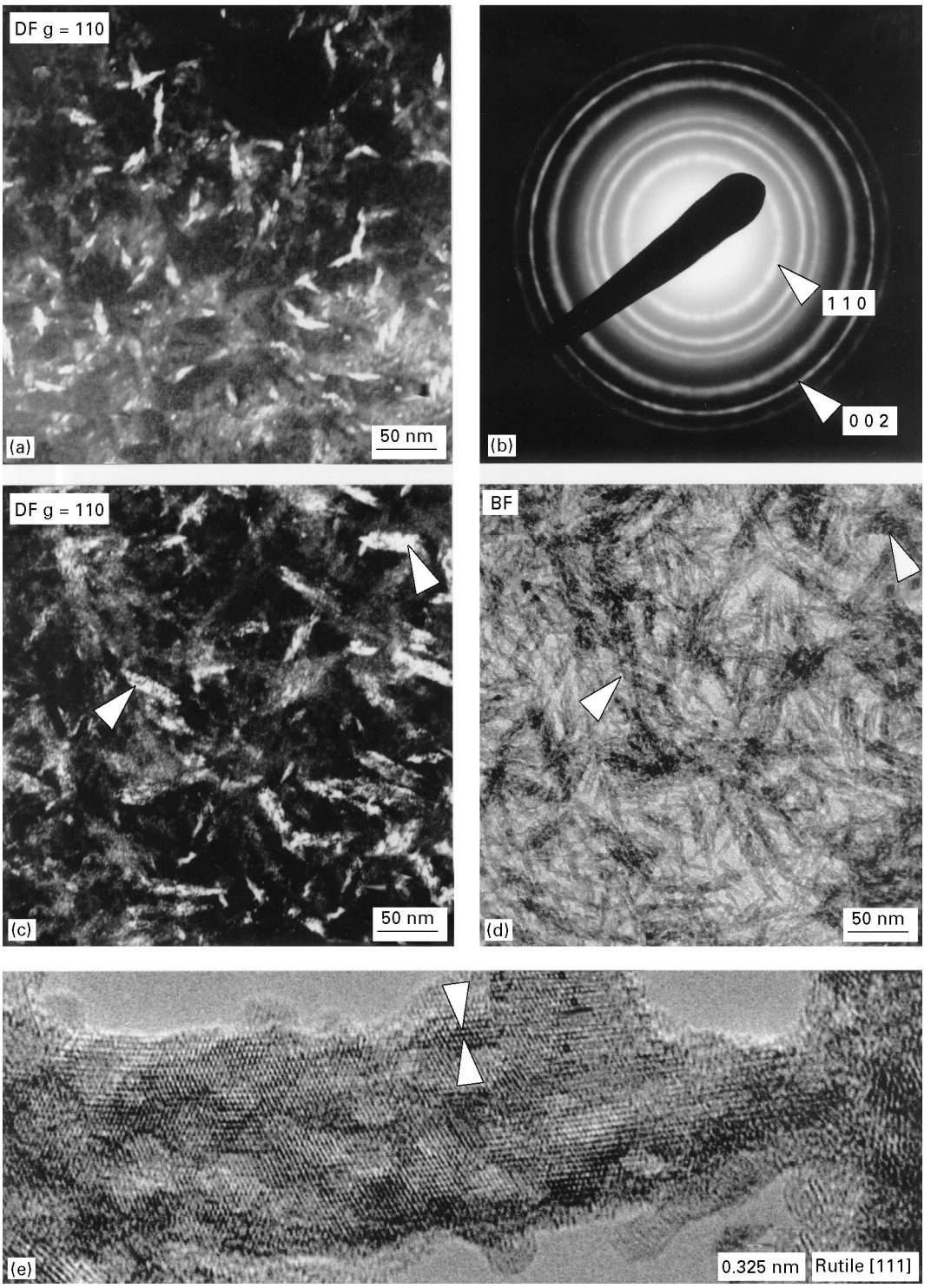

Figure 6 (a) A dark-field TEM image of needle-shaped precipitates after 2.5 h processing at 35 °C. The selected area diffraction pattern, (b), determines the precipitates have the rutile structure. (c) and (d) are a dark-field/bright-field pair, which shows that the precipitates have grown after 7.5 h at 35 °C, as compared to (a). (e) A high-resolution TEM image of a needle showing (1 1 0) fringes that are continuous for dimensions substantially longer than the size of the small crystallites ($\sim$3 nm).

concentration of alcohol was found not to affect the phase formed [39]. This is presumed to be due to the lack of significant participation of the alcohol in the condensation reaction at low pH. The condensation reaction can occur either by the elimination of water (HOH) or alcohol (ROH) depending on whether an OH or OR group is attached to the metal. At low pH, the number of OR groups attached to the metal are few; thus the majority of the condensation reaction occurs as a result of the water elimination reaction.

The anion (such as OH^-, O^{2-}, NO_3^-, SO_4^{2-}, etc.) has been observed to affect the phase and the morphology of oxide precipitates [40]. In the titania system, conflicting results have been reported showing that sulfate ions promote the formation of anatase [7] or that sulfate ions are necessary for the formation of rutile [10]. When nitrate anions are used, as in the present study, clearly either structure can be formed, with a dependence on temperature and pH. The role of the anion in the phase formation requires further clarification.

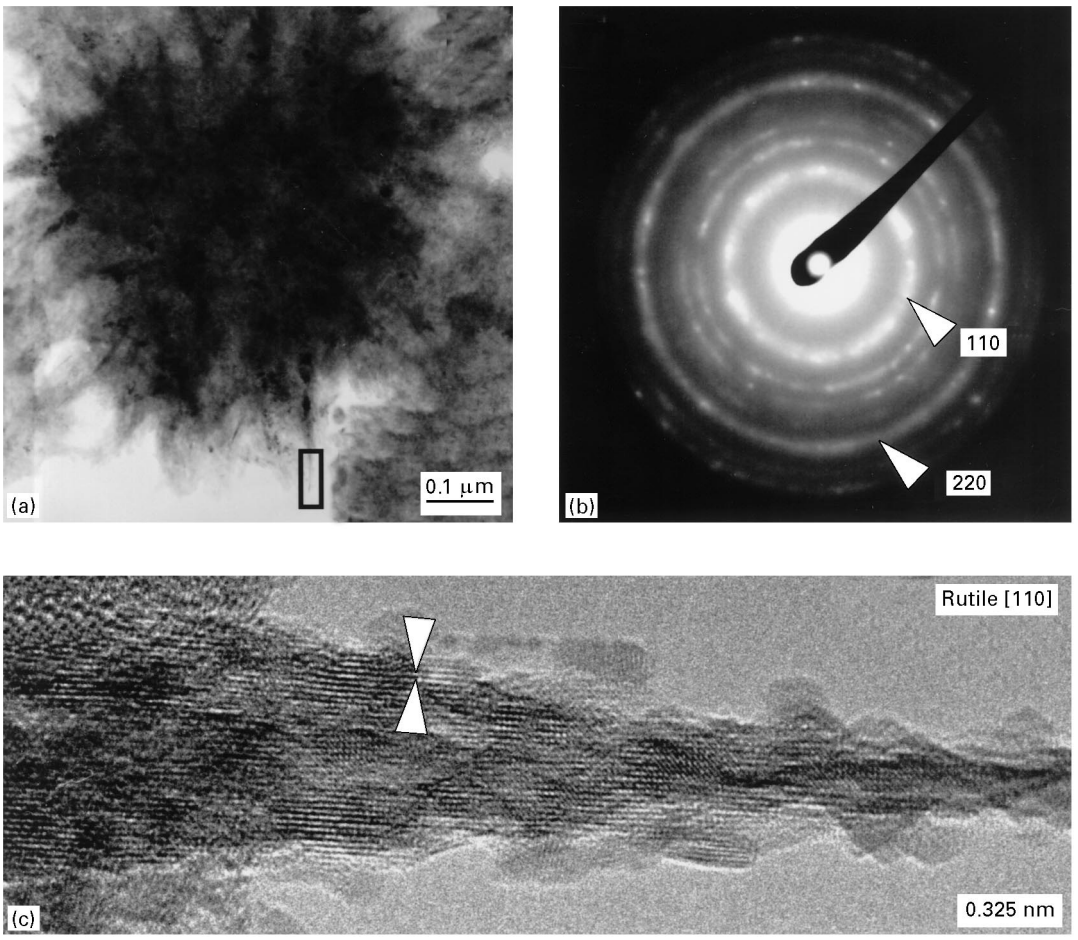

Figure 7 (a) A bright-field TEM image of a spherical cluster of needle-shaped precipitates of rutile. (b) A selected area diffraction pattern from a spheriod, showing it to be polycrystalline rutile. (c) A high resolution image of a single needle from the spheroid indicating the long-range crystalline order complicated by the non-continuous density of the needle.

The data presented above shows both the crystal structure and shape of the precipitate to be dependent on the reaction kinetics. This observation is consistent with the results obtained by others. A dependence on kinetics for the phase formed has been observed for the hydrolysis of $TiCl_4$ [41]. The nucleus of the product was determined to be anatase, whereas the surrounding crystal was rutile. It was suggested that the initial nucleation was fast and therefore formed anatase. The subsequent crystal growth was slower thereby allowing the formation of rutile.

The synthesis of anatase from titanium isopropoxide at low pH has been reported by O'Regan *et al.* [31]. The chemicals used by these workers are similar to those for the present study. However, they process their solution by quickly heating and holding the temperature at 80 °C, resulting in the formation of anatase. This condition is similar to the fast heating rate for the present study, which also produces anatase.

Both rutile and anatase were synthesized by Bekkerman *et al.* from aqueous solutions using titanium hydroxide as the starting precursor [12]. Titanium hydroxide [$Ti(OH)_4$] can be considered to be a titanium alkoxide [$Ti(OR)_4$] with the hydrogen atom replacing the alkyl group. To explain their synthesis, the authors proposed that the formation of anatase can be regarded as the interaction of two octahedral complexes by their vertices and that of rutile by their edges. However, anatase is a purely edge sharing structure with no corner sharing and rutile has both edge and corner sharing octahedra [32]. This implies that the model proposed by these workers does not correlate to the corresponding crystal structure. These workers also studied the effect of acid concentration on the phase formed. They found that higher acid concentrations promoted the formation of rutile and lower acid concentrations promoted anatase formation. In light of the model proposed in this study, the dependence of the phase formed on the acid concentration can be explained. The phase formed is governed by the rate of aggregation of the octahedral complexes. In the presence of acid, the aggregation processes are inhibited due to repulsion from adsorbed H^+ ions [14]. The higher the acid concentration, the larger the repulsion, and slower the aggregation. Hence, rutile is formed when the acid concentration is high. At higher pH, the repulsive forces are less, promoting faster aggregation and therefore the formation of anatase.

In addition to the hydrolysis of titanium isopropoxide (present study) and titanium hydroxide (described above), titanium chlorides and sulfates have been used to synthesize titanium dioxide [5–12]. In the presence of oxygen or water, it is thought that these precursors also undergo co-ordination expansion and

form 6-fold co-ordinated structures. Although the chemical species may differ, for all cases the titanium ion will be directly bonded to six oxygen atoms. These octahedral structures also undergo the condensation reaction to form precipitates. The rate at which this happens governs the phase formed, making all processes equivalent from a mechanistic view point.

4. Conclusions

A process has been developed to synthesize crystalline titanium dioxide powders from aqueous solutions at ambient temperatures ($T \leqslant 100\,^{\circ}\mathrm{C}$) and pressure. By controlling the reaction temperature, either the rutile phase or the anatase phase can be obtained.

The first stage, during which primary crystallites form, controls the phase formed. A slow reaction rate causes the formation of the thermodynamically favoured rutile phase. Faster reaction rates promote the formation of anatase. The second stage determines the morphology of the precipitates, which are formed by the aggregation of primary crystallites. Slow processing rates allow the primary crystallites (of rutile) to align and form needles up to 70 nm in length, which subsequently aggregate to form larger spheroids. For faster processing rates, the primary crystallites (of anatase) do not have sufficient time to align, and form featureless aggregates.

Acknowledgements

This work was supported by the Director, Office of Energy Research, Office of Basic Energy Sciences, Materials Sciences Division of the US Department of Energy, under contract No. DE-ACO3-76SF00098, and in part by the US Advanced Research Projects Agency under contract No. AO-8672. One of the authors (MG) would like to acknowledge partial financial support from the University of California in the form of the Regents Fellowship and James M. Goewey and Morris Boynton Lerned Fellowship.

References

1. *Ceramic Industry* **140** (1993) 37.
2. A. KAY and M. GRATZEL, *J. Phys. Chem.* **97** (1993) 6272.
3. M. A. ANDERSON, M. J. GIESELMANN and Q. XU, *J. Membrane Sci.* **39** (1988) 243.
4. K.-N. P. KUMAR, K. KEIZER, A. J. BURGGRAAF, T. OKUBO and H. NAGAMOTO, *J. Mater. Chem.* **3** (1993) 923.
5. A. KATO, Y. TAKESHITA and Y. KATATAE, *Mat. Res. Soc. Symp. Proc.* **155** (1989) 13.
6. J. S. REED, "Introduction to the principles of ceramic processing" (John Wiley, New York, 1988) p. 41.
7. M. KIYAMA, T. AKITA, Y. TSUSUMI and T. TAKADA, *Chem. Lett.* (1972) 21.
8. "Encyclopedia of chemical technology", vol. **23**, edited by H. F. Mark, D. F. Othmer, C. G. Overberger and G. T. Seaborg (John Wiley, New York, 1983) p. 139.
9. M. VISCA and E. MATIJEVIC, *J. Colloid Interface Sci.* **68** (1979) 308.
10. E. MATIJEVIC, M. BUDNIK and L. MEITES, *ibid.* **61** (1977) 302.
11. E. A. BARRINGER and H. K. BOWEN, *J. Amer. Ceram. Soc.* **65** (1982) C199.
12. L. I. BEKKERMAN, I. P. DOBROVOL'SKII and A. A. IVAKIN, *Russ. J. Inorg. Chem.* **21** (1976) 233.
13. C. J. BRINKER and G. W. SCHERER "Sol–gel science" (Academic Press, Boston, 1990) p. 21.
14. J. LIVAGE, M. HENRY and C. SANCHEZ, *Prog. Solid State Chem.* **18** (1988) 259.
15. B. E. YOLDAS, *J. Non-Cryst. Solids* **63** (1984) 145.
16. *Idem., J. Mater. Sci.* **14** (1979) 1843.
17. *Idem., ibid.* **21** (1986) 1087.
18. B. D. FABES and D. R. UHLMANN, in "Innovations in materials processing using aqueous, colloid and surface chemistry", edited by F. M. Doyle, S. Raghavan, P. Somasundaran and G. W. Warren (TMS, Warrendale, PA, 1988) p. 127.
19. K. D. KEEFER, in "Better ceramics through chemistry", edited by C. J. Brinker, D. E. Clark and D. R. Ulrich, (Materials Research Society, Pittsburgh, PA, 1984) p. 15.
20. A. NAZERI and M. KAHN, *Amer. Ceram. Soc. Bull.* **72** (1993) 59.
21. B. E. YOLDAS, *ibid.* **54** (1975) 286.
22. "Phase diagrams for ceramists", edited by E. M. Levine and H. F. McMurdie (American Ceramic Society, Westerville, OH, 1975) Fig. 4258.
23. A. NAVROTSKY and O. J. KLEPPA, *J. Amer. Ceram. Soc.* **50** (1967) 626.
24. ATOMS software
25. R. C. WEAST (ed.), "Handbook of chemistry and physics" (CRC Press, Boca Raton, FL, 1984) B-154.
26. T. ZOLTAI and J. H. STOUT, "Mineralogy: concepts and principles" (Burgess Publishing Co., Minneapolis, MN, 1984) p. 411.
27. J. LIVAGE and M. HENRY, in "Ultrastructure processing of advanced ceramics", edited by J. D. Mackenzie and D. R. Ulrich (John Wiley, New York, 1988) p. 187.
28. J. R. BARTLETT and J. L. WOOLFREY, in "Chemical processing of advanced materials", edited by L. L. Hench and J. K. West (John Wiley, New York, 1992) p. 247.
29. Q. J. WANG, S. C. MOSS, M. L. SHALZ, A. M. GLAESER, H. W. ZANDBERGEN and P. ZSCHACK, in "Physics and chemistry of finite systems: from clusters to crystals", Vol. II, edited by P. Jena, S. N. Khanna and B. K. Rao (Kluwer Academic Publishers, Boston, 1992) p. 1287.
30. L. H. EDELSON and A. GLAESER, *J. Amer. Ceram. Soc.* **71** (1988) 225.
31. B. O'REGAN, J. MOSER, M. ANDERSON and M. GRÄTZEL, *J. Phys. Chem.* **94** (1990) 8720.
32. L. PAULING, *J. Amer. Chem. Soc.* **51** (1929) 1010.
33. P. MEAKIN, in "Kinetics of aggregation and gelation", edited by F. Family and D. P. Landau (North Holland Physics Publishing, New York, 1984) p. 91.
34. P. PIERANSKI, *Contemp. Phys.* **24** (1983) 25.
35. E. A. HAUSER and D. S. LE BEAU, *J. Phys. Chem.* **42** (1938) 961.
36. J. H. L. WATSON, W. HELLER and W. WOJTOWICZ, *Science* **109** (1949) 274.
37. W. HELLER, in "Polymer colloids II", edited by R. M. Fitch, (Plenum Press, New York, 1980) 153.
38. A. BLEIR and R. M. CANNON in "Better ceramics through chemistry II", edited by C. J. Brinker, D. E. Clark and D. R. Ulrich (Materials Research Society, Pittsburgh, PA, 1986) p. 71.
39. M. GOPAL, M.S. thesis, University of California at Berkeley, (1994).
40. E. MATIJEVIC, *Acc. Chem. Res.* **14** (1981) 22.
41. T. IIDA, K. YAMAOKA, S. NOZIRI and H. NOZAKI, *Kogyo Kagaku Zasshi* **69** (1966) A 118 (English abstract).

Received 7 May 1996
and accepted 22 May 1997